Synthesis of Novel Thin-Film Materials by Pulsed Laser Deposition
Author(s): Douglas H. Lowndes, D. B. Geohegan, A. A. Puretzky, D. P. Norton and C. M. Rouleau
Reviewed work(s):
Source: *Science*, New Series, Vol. 273, No. 5277 (Aug. 16, 1996), pp. 898-903
Published by: American Association for the Advancement of Science
Stable URL: http://www.jstor.org/stable/2891510
Accessed: 12/07/2012 12:02

Your use of the JSTOR archive indicates your acceptance of the Terms & Conditions of Use, available at http://www.jstor.org/page/info/about/policies/terms.jsp

JSTOR is a not-for-profit service that helps scholars, researchers, and students discover, use, and build upon a wide range of content in a trusted digital archive. We use information technology and tools to increase productivity and facilitate new forms of scholarship. For more information about JSTOR, please contact support@jstor.org.

*American Association for the Advancement of Science* is collaborating with JSTOR to digitize, preserve and extend access to *Science*.

http://www.jstor.org

25. P. V. Braun, P. Osenar, S. I. Strupp, *Nature* **380**, 325 (1996).
26. A. Monnier *et al.*, *Science* **261**, 1299 (1993); A. Firouzi *et al.*, *ibid.* **267**, 1138 (1995); C. H. Chen, S. L. Burkett, H. X. Li, M. E. Davis, *Microporous Mater.* **2**, 27 (1993).
27. H. Yang *et al.*, *Nature* **379**, 703 (1996).
28. S. Manne *et al.*, *Langmuir* **10**, 4409 (1994); ——— and H. Gaub, *Science* **270**, 1480 (1995).
29. The procedure involves dissolving TEOS liquid in an aqueous solution of CTAC and hydrochloric acid. Typical molar ratios are 1 TEOS:2 CTAC:9.2 HCl: 1000 $H_2O$. Under these solution conditions, mesoscopic silica films spontaneously grow onto substrates in contact with the liquid.
30. Under similar conditions, freestanding mesostructured silica films can also be grown at the air/water interfaces [H. Yang *et al.*, *Nature* **381**, 589 (1996); and work at Princeton University by N. Nakagawa *et al.*, unpublished results].
31. To obtain these images, we used a method described in (*28*) and (*32*) that uses electrical double layer repulsive forces to image the charge distribution of an adsorbed layer on the sample. The images of the outer layer of the reacting mesostructured film were obtained by immersing the imaging tip and substrate in the reacting mixture and, once sufficient time was allowed for thermal and mechanical equilibration, setting the imaging setpoint in the repulsive precontact region. In this way, the tip is held ~1 nm above the reacting surface and the scanning motion of the AFM produces a topological map of charge density.
32. T. J. Senden, C. J. Drummond, P. Kekicheff, *Langmuir* **10**, 358 (1994).
33. After 10 hours of reaction, in situ AFM images are difficult to obtain because of the appreciable growth of mesostructured silica on the top surface of the AFM flow cell and cantilever spring. The presence and irregular nature of both of these films disturb the reflection of the laser light beam used to monitor spring deflection.
34. AFM studies on systems containing only surfactant, with no TEOS, reveal the presence of several layers of adsorbed surfactant tubules. Three-dimensional "multilayer" features have been imaged with the microscope, and as many as three "steplike" features are observed in the repulsive portion of the force-distance curve near the substrate (M. Trau *et al.*, in preparation). The existence of such supramolecular surfactant structures in the absence of TEOS suggests a sequential reaction mechanism involving surfactant self-assembly followed by inorganic condensation.
35. Y. Gao, J. Du, T. Gu, *J. Chem. Soc. Faraday Trans. 1* **83**, 2671 (1987); B.-Y. Zhu and T. Gu, *ibid.* **85**, 3813 (1989); T. Gu and Z. Huang, *Colloids Surf.* **40**, 71 (1989); J. Leimbach and J. S. H. Rupprecht, *ibid.* **94**, 1 (1995).
36. W. Z. Helfrich, *Naturforchung* **28C**, 693 (1973).
37. S. M. Gruner, *J. Phys. Chem.* **93**, 7562 (1989); R. P. Rand *et al.*, *Biochemistry* **29**, 76 (1990).
38. We observed +18% strain in the film grown in the nonequilibrium condition, in the case where the solution is confined in a thin film geometry by a wrap. We found that the film grows about an order of magnitude faster in this condition. A striking feature of our data is that there is a large change in the Bragg peak position as these films dry that corresponds to large changes in the film lattice constant and strain. For example, the degree of hexagonal strain varies from +18% while wet to +2% a few hours after removal from solution, and finally −7% several days later when they are dry. In this process, the lateral spacings of the film increased by 2% upon drying and finally by 5% after a few days. This implies that the 25% change in *a*/*b* ratio of the film upon drying is largely due to a change in the vertical lattice spacings due to drying shrinkage in the normal direction.
39. This work was supported by the U.S. Army Research Office (grant DAAH04-95-1-0102) and MRSEC program of the NSF (DMR-940032). We thank D. M. Dabbs for useful discussions and help in the manuscript preparation and Digital Instruments for technical support.

# Synthesis of Novel Thin-Film Materials by Pulsed Laser Deposition

Douglas H. Lowndes, D. B. Geohegan, A. A. Puretzky, D. P. Norton, C. M. Rouleau

**Pulsed laser deposition (PLD) is a conceptually and experimentally simple yet highly versatile tool for thin-film and multilayer research. Its advantages for the film growth of oxides and other chemically complex materials include stoichiometric transfer, growth from an energetic beam, reactive deposition, and inherent simplicity for the growth of multilayered structures. With the use of PLD, artificially layered materials and metastable phases have been created and their properties varied by control of the layer thicknesses. In situ monitoring techniques have provided information about the role of energetic species in the formation of ultrahard phases and in the doping of semiconductors. Cluster-assembled nanocrystalline and composite films offer opportunities to control and produce new combinations of properties with PLD.**

The first PLD experiment was carried out more than 30 years ago, shortly after the invention of the pulsed ruby laser (*1*). However, it was only during the past decade that PLD received extensive experimental development and came into widespread use for film-growth research. The impetus was the discovery that high-quality high-temperature (high-$T_c$) superconductor (HTS) films can be grown in a low-pressure oxygen environment by PLD without the need for further processing (*2*). This discovery opened the field of oxide ceramic film growth and research to PLD; in turn, PLD has invigorated and enriched the oxide field. During the past 9 years, PLD's advantages for the deposition of oxides and other complex materials have been used to grow films with an enormous variety of properties, including ferroelectrics, ferrites, amorphous diamond and other ultrahard phases, biocompatible and tribological coatings, polymers, compound semiconductors, and nanocrystalline materials (*3*).

This article describes the ablation process and its characteristic advantages and limitations for film deposition. Three themes in contemporary PLD research then are examined: (i) the creation of artificial structures and metastable phases and the systematic variation of their properties, (ii) information about the role of energetic ablated species in the formation of ultrahard phases and in the doping of semiconductors, and (iii) emerging opportunities in the synthesis of nanocrystalline and composite thin-film materials with PLD.

D. H. Lowndes, D. B. Geohegan, D. P. Norton, and C. M. Rouleau are in the Solid-State Division, Oak Ridge National Laboratory, Post Office Box 2008, Oak Ridge, TN 37831–6056, USA. A. A. Puretzky is at the Institute of Spectroscopy, Russian Academy of Sciences, Troitsk, Russia.

## Pulsed Laser Ablation

Although the underlying ablation process is complex, PLD is conceptually and experimentally simple. An ultraviolet (UV) pulsed laser beam (pulse duration, 10 to 50 ns) is focused with an energy density $E_d$ of 1 to 5 J/cm$^2$ onto a rotating polycrystalline target (Fig. 1). Several events occur during the laser pulse: rapid heating and vaporization of the target; increasing absorption by the vapor until breakdown occurs to form a dense plasma; and absorption of the remainder of the laser pulse to heat and accelerate the plasma, which contains neutral atoms, molecules, and ions, in both ground and excited states, as well as energetic electrons. The atoms and ions undergo collisions in the high-density region near the target (the Knudsen layer, which is a few hundred micrometers thick) to create a highly directional expansion perpendicular to the target surface with initial velocities $\geq 10^6$ cm/s. If ablation is carried out in a low-pressure reactive gas such as oxygen, simple oxide molecules are also formed in the expanding ablation beam. In an ambient gas, a shock front results from collisions between the expanding plasma and the gas molecules (Fig. 2). This front propagates with gradu-

ally decreasing velocity (4) toward a heated substrate, typically 5 to 10 cm away, on which film growth occurs. Amorphous, polycrystalline, or epitaxial single-crystal films can be grown, depending on the nature of the substrate and its temperature.

## Characteristics of Pulsed Laser Deposition

PLD has several characteristics that distinguish it from other film-growth methods and provide special advantages for the growth of oxides and other chemically complex (multielement) materials.

*Congruent (stoichiometric) transfer of material.* Films have the same composition as the target when the focused laser energy density is chosen properly. Congruent transfer is a consequence of the high initial rate of heating and highly nonthermal target erosion by a laser-generated plasma. It sets PLD apart from incongruent-transfer methods such as thermal evaporation or sputtering.

*Deposition from an energetic plasma beam.* In the ablation "plume" (Fig. 2), atoms and ions have typical initial velocities of $\geq 10^6$ cm/s, which for an atom of 100 atomic mass units corresponds to a kinetic energy $\geq 52$ eV. The kinetic and internal excitation energies of ablated species can be used to assist film formation and to promote chemical reactions, both in the gas phase and on the growing film surface.

*Capability for reactive deposition in ambient gases.* No electron beams or hot filaments are needed in the deposition chamber (Fig. 1), so ambient gases can be used. Energetic species in the ablation plasma react readily with gas molecules to form simple compounds (oxides, nitrides, and hydrides). Reactive deposition in low-pressure oxidants such as $O_2$, $O_3$, $NO_2$, $N_2O$, or water vapor, in combination with the congruent-transfer property, allows the growth of high-quality thin films of previously difficult-to-fabricate multicomponent ferroelectric, ferrite, and biocompatible oxide ceramic materials by PLD.

*Growth of multilayered epitaxial heterostructures.* In these thin-film structures, adjacent layers have different compositions, but all layers share a common, continuous crystal structure. A separate target can be used to grow each layer, with a multitarget "carousel" for rapid target exchange. Growth is inherently "digital" because each layer's thickness can be controlled precisely simply by calibrating the deposition rate per laser pulse and counting pulses. By choosing a low deposition rate (such as 0.1 Å per pulse), it is possible to control film growth near the atomic layer level. By increasing the laser pulse rate, one can maintain attractive overall growth rates. With the use of multiple multielement targets, artificial superconducting superlattices (5) and elegant prototype superconducting device structures (6) have been grown by PLD.

The ablation process has two characteristics that have limited its use, especially for semiconductors and other electronic thin-film materials.

*Particulates.* Particulates with diameters ranging from ~0.1 to ~10 μm (with most ≤1 μm) usually are present in PLD films (7). They are of particular concern if films must be lithographically patterned on a micrometer or smaller scale. Both "passive" and "active" experimental techniques have been developed to minimize the number and size of particulates. The most important passive methods are to use a short-wavelength laser (such as a deep-UV excimer) and to "condition" the target to maintain a smooth surface (by a combination of target rotation and laser beam scanning). The most effective active method is to use a rotating-vane "velocity filter" to intercept most of the massive and relatively slow-moving particulates while transmitting the high-velocity atomic and ionic flux (7).

*Uniform thickness films.* A tightly focused pulsed laser beam produces a distribution of ablated material that is strongly peaked in the forward direction (Fig. 2); therefore uniform thickness films are produced only in a relatively narrow angular range. The practical solution to this problem is to move the ablation plume relative to the substrate, "painting" the substrate with the plume. For example, the laser beam can be raster-scanned over the target (8), the substrate can be rotated under an offset plume, or these motions can be combined to obtain uniform thickness depositions. Greer and Tabat (9) showed that laser beam rastering over a large diameter target can produce uniform, large area films with predictable and reproducible growth rates and properties. For example, oxide ceramic films have been deposited over 150-mm-diameter substrates, with variations of only ±2.3% and ±0.5% for thickness and composition, respectively.

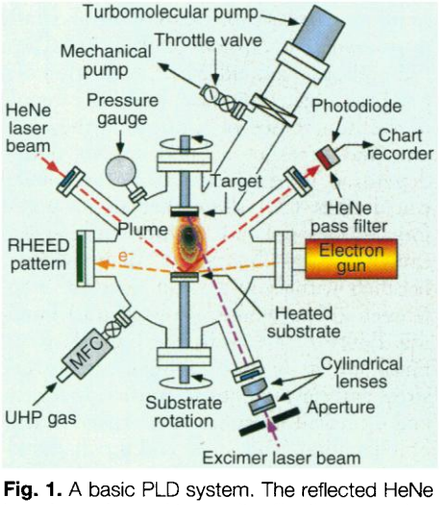


**Fig. 1.** A basic PLD system. The reflected HeNe laser beam is used to monitor film thickness during deposition in a reactive gas. Reflection high-energy electron diffraction (RHEED) is used to monitor surface crystallinity and quality (intermittently in a gas or continuously in vacuum). UHP, ultrahigh purity; MFC, mass flow controller.

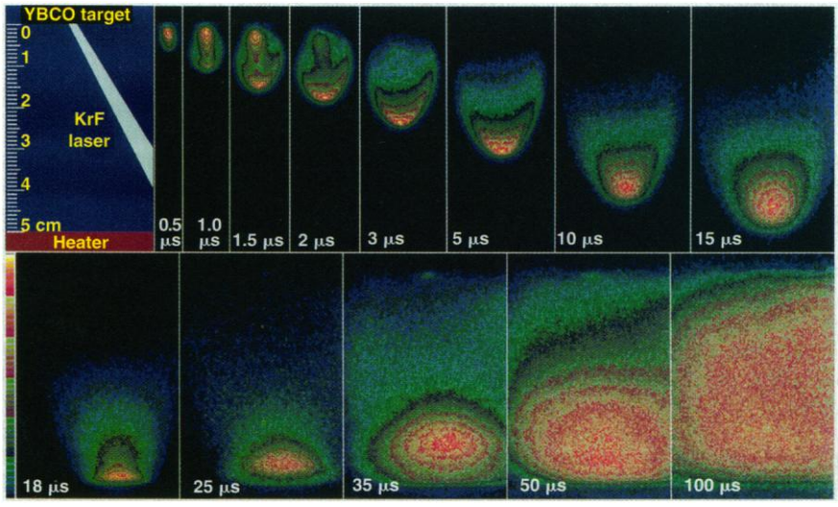


**Fig. 2.** Gated, intensified CCD-array photographs of the total visible-light emission from the laser-generated plasma after 2.5 J/cm² KrF laser ablation of $YBa_2Cu_3O_{7-x}$ into 200 mtorr of $O_2$, at the indicated delay times after arrival of the laser pulse. The digitized intensity data have been divided equally into six contours (indicated by the palette at the left) in order to reveal the fainter emitting regions. Exposure times were increased from 20 ns to 2 μs. The plasma "plume" collides with the (cold) substrate heater plate in the final frames, partially rebounding to fill the target-heater space at long times.

## Liquid Targets and Dual-Laser Ablation

A dual-laser ablation technique was developed recently in which initial target heating by a pulsed $CO_2$ laser (wavelength, 10.6 μm) produces a shallow, transient molten layer, from which a slightly time-delayed pulsed excimer laser then initiates the ablation plasma plume (*10*). Ablation from the momentarily liquid target has resulted in a thousandfold reduction in particulate density in $Y_2O_3$ films (*10, 11*). Moreover, the highly efficient heating of the excimer-generated plasma by the tail end of the $CO_2$ laser pulse produces an ablation plume that is much more highly excited, and has a greatly broadened angular distribution, compared with the plume produced by an excimer pulse alone (*10*). Thus, dual-laser ablation is a promising technique to simultaneously minimize both particulates and the angular distribution problem.

## Artificial HTS and Oxide Electronics

Thin-film growth methods allow one to make new materials by creating artificially layered crystal structures. The surfaces of single-crystal substrates provide atomic templates that can be used to constrain atomic positions and thereby stabilize epitaxial films in crystal structures that are only metastable; in this way, thin films can be locked into structures that cannot be achieved by bulk processing methods near thermodynamic equilibrium. Pulsed laser deposition is particularly attractive for the formation of artificially layered oxides because material can be transferred stoichiometrically in the presence of reactive background gases such as oxygen.

The cuprate superconductors are ideal candidates for studies of the formation of artificially layered compounds because all of the highest $T_c$ compounds are inherently layered materials based on an oxygen-deficient perovskite structure (such as $SrTiO_3$). Different HTS compounds contain different numbers of $CuO_2$ sheets within their unit cells, separated by chemically different "spacer" or charge reservoir layers; they are ceramic superlattices. (A superlattice material is constructed to have properties, such as composition, that are periodically modulated on a length scale longer than the crystallographic unit cell dimensions.) Recognition of this common structural feature immediately suggested the possibility of recreating bulk-material HTS phases in thin-film form—and of going beyond to create entirely new "artificial" HTS—by controlling the stacking sequence of various oxide layers at nearly the atomic level.

The simplest compound containing $CuO_2$ planes is the "infinite layer" material $XCuO_2$, whose structure consists simply of sheets of alkaline earth atoms (X = Ca, Sr, or Ba) alternating with $CuO_2$ layers. By using "laser molecular beam epitaxy (MBE)" growth techniques to insert infinite layer (Ca,Sr)$CuO_2$ modules, researchers have extended metastable thin-film structures of the $Bi_2Sr_2Ca_{n-1}Cu_nO_{2n+4}$ phases to $n = 8$, well beyond the $n = 1$, 2, and 3 that are readily obtained by bulk processing (*12*). In addition, entirely new families of artificially layered HTSs have been formed as $BaCuO_2$/(Ca,Sr)$CuO_2$ superlattices based on the infinite layer structure (*13, 14*). By sequentially ablating $BaCuO_2$ and (Ca,Sr)$CuO_2$ targets, the (Ca,Sr)$CuO_2$ and $BaCuO_2$ "building blocks" were epitaxially stabilized in the infinite layer structure and found to have superconducting transition temperatures as high as $T_c$(onset) ~ 70 K (*14*). The significance of these results is that a new family of superconductors was synthesized by the assembly of a "superlattice compound" from $SrCuO_2$, an insulator, and $BaCuO_2$, which normally does not exist in the infinite layer structure, even with the use of high-pressure synthesis techniques (*14*).

The HTS materials are only a small subset of the much larger family of oxide and nitride materials whose members exhibit an enormous range of physical properties. The possibility of creating artificially engineered "ceramic superlattice" thin-film materials—with enhanced magnetic, ferroelectric, and even semiconducting properties through control of layer thickness and spacing—is only now beginning to be explored. Recently, relatively simple wet etching or thermal annealing techniques, or both, have been used to prepare substrates such as $SrTiO_3$ and $Al_2O_3$ with atomically flat terraces (*15*). Monitoring of both surface composition (*15*) and film thickness (*15, 16*) can be carried out with atomic layer accuracy during laser MBE oxide film growth. Strained dielectric superlattices of $BaTiO_3$ and $SrTiO_3$ formed by PLD (*17, 18*) have strikingly different electrical properties than the solid solution (Sr,Ba)$TiO_3$ (*17*). The epitaxial growth of other insulating and ferroelectric artificially layered materials such as $KNbO_3$/$KTaO_3$ superlattices has been reported as well (*19*).

The formation of oxide superlattice thin-film structures is a promising approach to study the effects of strain on useful macroscopic properties in order to further tailor properties. Pulsed laser deposition is being used to synthesize heterostructure ferroelectric capacitors equipped with conductive oxide electrodes for use in ferroelectric thin-film memory technology and eventual integration with Si complementary metal-oxide-semiconductor (CMOS)–based electronics (*20*). In fact, the possibility of creating an entirely new field of oxide-based optoelectronics is the subject of a report currently being prepared by a team of industrial and academic researchers in Japan (*21*).

Pulsed laser deposition also was responsible for the recent discovery of colossal magnetoresistance (CMR) in $La_{0.67}Ca_{0.33}MnO_x$ films that are both magnetic and electrically conducting (*22*). After suitable heat treatment, $La_{0.67}Ca_{0.33}MnO_x$ films grown epitaxially on $LaAlO_3$ substrates exhibit negative magnetoresistance [$MR = \Delta R/R_H = (R_H - R_0)/R_H$, where $R_z$ is resistance in field z] that is more than four orders of magnitude larger (*22, 23*) than the typical giant magnetoresistance found previously in metallic multilayer films (*24*). In a magnetic field of 6 T, the resistance of ~1000 Å thick $La_{0.67}Ca_{0.33}MnO_x$ films decreases by more than 10,000-fold at a temperature near 110 K, with most of the change occurring at low fields (*23*). The strong dependence of the MR ratio on film thickness has been ascribed tentatively to the effects of lattice strain on the exchange interaction between manganese ions, but current research is focused on understanding the origins of CMR in $La_{0.67}Ca_{0.33}MnO_x$ and related materials (*23*). Colossal MR is expected to be useful for magnetic and electronic device applications when the effects of strain and material processing are better understood (*22*).

## The Role of Energetic Ablated Species

*Synthesis of "amorphous diamond" films.* The room-temperature synthesis of tetrahedrally coordinated amorphous carbon (ta-C, or "amorphous diamond") by the ablation of a graphite target provides a striking example of the importance of controlling the energies and types of ablated species during deposition. Experiments (*25–31*) and model calculations (*32*) show that in its purest form, disordered ta-C exhibits almost entirely $sp^3$ (tetrahedral, or diamond-like) bonding with only a small fraction of $sp^2$ (threefold-coordinated or graphitic) bonding. Films of ta-C with the highest $sp^3$:$sp^2$ ratios are in a state of high compressive stress and have values of density, hardness, and electrical resistance near those of natural diamond. This stress and the diamond-like bonding are thought to result from the shallow implantation of energetic carbon ions during film formation, which drives the effective temperature and pressure conditions to exceed the values needed to form the stable diamond phase (*25*).

Two vapor deposition processes, filtered

vacuum arc deposition (*25*, *26*) and PLD (*27*–*31*), have proven the most successful for ta-C film growth because of their ability to supply energetic particle fluxes in the range from 10 to 100 eV (*28*). Absorption of photons by free electrons in a plasma is most effective at longer wavelengths, so initial PLD experiments used near-infrared Nd:yttrium-aluminum-garnet (1064 nm) lasers focused to extremely high intensities ($0.5 \times 10^{11}$ to $5.0 \times 10^{11}$ W/cm$^2$) to produce ta-C films with ~40 to 70% $sp^3$ bonding (*30*, *31*). These films are good field emitters, and this process has been commercially developed for the production of flat panel displays (*33*). However, short-wavelength (193 nm), nanosecond ArF excimer lasers subsequently have proven to be far superior at maximizing the $sp^3$ bonding (at 84 to 95%) while using much lower laser intensities of less than $5 \times 10^8$ W/cm$^2$ (*30*, *31*).

The reason for this strong laser-wavelength dependence of the $sp^3$:$sp^2$ ratio was understood only recently when gated photon-counting spectroscopy was combined with spectroscopic imaging to obtain temporally and spatially resolved images of the evolution of the species present in the ablation plume (*31*, *34*). When KrF (248 nm) and ArF (193 nm) excimer laser wavelengths were used to irradiate graphite targets at equal intensities, quite different proportions of the energetic ions needed for ta-C formation and of slower-moving clusters were found. In fact, images of the visible plume luminescence revealed three distinct components to the transport at the high laser intensities where ta-C films are grown. These regions, and their temporal evolution, then were identified by emission and absorption spectroscopy at different laser intensities.

All three components are visible in Fig. 3, which compares the plumes generated by KrF and ArF ablation at equal focused energy densities. (i) At low laser intensity, only a slowly propagating component of luminescence is seen. It contained carbon dimers ($C_2$), trimers ($C_3$), and higher clusters ($C_n$) with low kinetic energy (KE); for example, KE($C_3$) ~ 0.2 to 1.7 eV. (ii) At intermediate laser intensity, a second, broader ball of luminescence explodes from the slow-moving clusters to travel at a velocity $v_{center}$ ~ 1.0 cm/μs. This emission was identified as coming from atomic carbon neutrals [KE(C) ~ 6 eV]. (iii) As the laser intensity is further increased, a very fast ball of luminescence from $C^+$ ions forms and accelerates on the leading edge of the expanding plume, with $v_{center}$ ~ 3.7 cm/μs and KE ~ 85 eV. The ArF plume is dominated by this fast component, whereas the KrF plume exhibits only weak luminescence from this region.

Correlation of the relative amounts of these three plume components with the properties of diamond-like films showed that an increase in laser intensity (at either wavelength) resulted in increased luminescence of the energetic third component relative to the first, as well as more diamond-like films (*34*). The time evolution of the three components shows that deep-UV photons couple more of their energy into the plume by breaking up clusters and ionizing atoms than by heating the electrons. This conversion of the slow-cluster component of the plume into fast ions by the strong absorption of short-wavelength photons appears to be the fundamental factor controlling the diamond-like quality of ta-C films.

*Semiconductor growth and doping.* The stoichiometric-transfer property of PLD makes it potentially attractive for the growth of chemically complex semiconductors. For instance, the currently underutilized direct-gap quaternary and pentenary chalcopyrites (prototype: $CuIn_{1-x}Ga_xSe_2$) could provide a rich variety of energy band gaps and lattice constants for photovoltaic and optoelectronic devices. Depositing films in reactive environments is intriguing as well for growing semiconducting group-III nitride alloys such as $Ga_{1-x-y}In_xAl_yN$ (*35*) and for controlling semiconductor electrical properties by deliberately introducing dopant atoms from the gas phase.

The feasibility of gas-phase doping during ablation was explored recently: a ZnTe target was ablated through molecular $N_2$. Highly *p*-type ZnTe films with hole concentrations $p \sim 10^{20}$ cm$^{-3}$ were grown on GaAs(001) substrates (*36*–*38*). The x-ray diffraction measurements revealed a ~0.4% decrease in lattice constant, consistent with the substitution of relatively small N (group V) ions onto Te (group VI) sites to produce the *p*-type conductivity. However, the hole mobility (a measure of the scattering of the hole carriers by defects) was sharply peaked at a $N_2$ pressure of ~50 mtorr (~6.7 Pa) during ablation (*36*–*38*).

In order to understand the $N_2$ pressure dependence of the mobility, time-resolved ion current measurements (*39*) were carried out during the ablation of ZnTe into $N_2$, with the ion probe located at the position of the GaAs substrate (*37*, *38*). Three distinct peaks (or "modes" of incident species) were observed as a function of $N_2$ pressure (Fig. 4). The fast peak (labeled "1" in Fig. 4) contains ions that have suffered no collisions with ambient $N_2$ molecules. These ions have KEs sufficient to displace atoms from crystal lattice sites, producing defects that will scatter carriers. The flux of these fast ions is attenuated exponentially with increasing $N_2$ pressure, but some remain

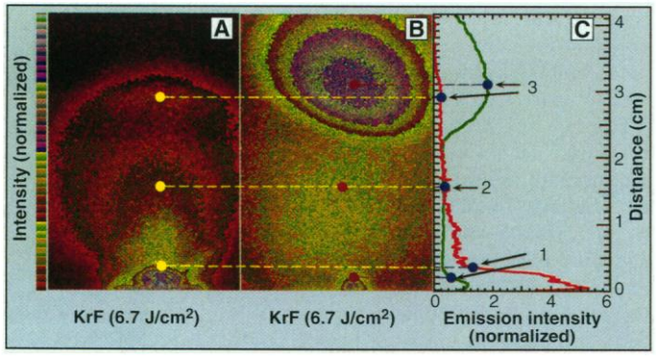


**Fig. 3.** Gated, intensified CCD-array photographs of the total visible luminescence 800 to 850 ns after ablation of pyrolytic graphite in vacuum by (**A**) a KrF laser and (**B**) an ArF laser, both at focused energy densities of 6.7 J/cm$^2$. The laser beam is incident at 30° to the right of the target surface normal, as shown in the leftmost panel of Fig. 2. The intensity of the emission is represented by the palette shown at the left, normalized to the maximum numbers of counts for each image. (**C**) A line-plot profile from the irradiated spot outward along the target normal for the (red) KrF laser and the (green) ArF laser showing the relative intensities of the different plasma components: (1) the slow cluster component near the target surface, (2) the faster moving component of atomic emission, and (3) the fast, ball-shaped ionic component. The line profiles are normalized to the intensity of the second component.

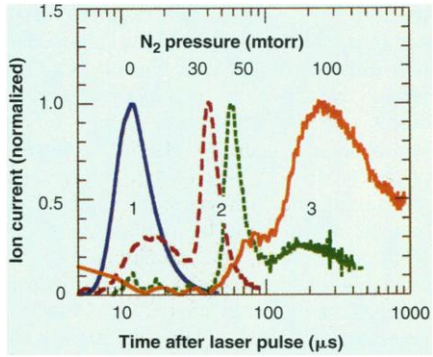


**Fig. 4.** Ion current versus time at a distance of 10 cm from a ZnTe target after ablation into $N_2$ gas at various pressures. The labels 1, 2, and 3 refer to three "modes" of incident species, namely unscattered ions, ions that are slowed by gas-phase collisions, and slow-moving clusters formed through collisions, respectively.

until the pressure reaches ~50 mtorr (Fig. 4). Mode 2, the dominant part of the ion current for $N_2$ pressures between ~15 and ~70 mtorr, is due to ions that have been slowed by collisions with $N_2$ molecules. These ions arrive at the substrate with KEs of only a few electron volts or less, which is nearly ideal to promote chemical reactions in the near-surface region but well below the threshold for lattice displacement damage. A third contribution (labeled "3" in Fig. 4) dominates the ion probe signal for $N_2$ pressures $\geq$ 70 mtorr, the pressure range for which the hole mobility declines. The mode 3 peak represents very slow-moving species; in fact, its emergence marks the onset of significant cluster formation by means of gas-phase collisions in the increased $N_2$ pressure. High-resolution transmission electron microscopy (TEM) images obtained from a cross section of ZnTe films grown at 100 mtorr revealed a transition to columnar growth, with both the film surface and near-surface intergranular regions decorated with spherical particles that have diameters of ~9.5 to 17 nm, apparently grown from the clusters of mode 3 (*37*).

Thus, combined ion current and TEM measurements reveal transitions, controlled by the $N_2$ pressure, between regimes in which different species are present in the incident ablation flux. The peak in hole mobility apparently results from the competition between defect production at low $N_2$ pressures and the onset of significant cluster deposition for higher $N_2$ pressures. The highest hole mobility is achieved for growth from incident ions and atoms with KEs of only a few electron volts.

## Cluster Formation: Nanocrystalline and Composite Films

Cluster formation can be greatly enhanced by ablating a material into a moderate-pressure (~1 torr) gas. For example, when carbon (graphite) is ablated into argon, carbon dimers, trimers, and clusters ($C_n$) are formed by collisions of energetic carbon atoms and ions (*34*). By ablating a binary semiconductor such as InP, mixed clusters of the type $In_mP_n$ result (*40*); if a reactive gas is used, the clusters contain both target and gas atoms. Thus, by increasing the ambient gas pressure, one can change the flux available for film deposition from primarily energetic atoms and ions to one that includes small clusters. Eventually, significant numbers of nanocrystals are formed, typically with diameters of 1 to 10 nm and containing $10^2$ to $10^5$ atoms.

Highly nanocrystalline or cluster-assembled films typically have properties much different from films grown with the use of a predominantly atomic or ionic flux, either because of quantum confinement effects (in very small crystallites) or because entirely new, composite materials are formed. For example, self-supporting thin films of agglomerated Si nanocrystals recently were created by ablating a Si rod while simultaneously flowing high-pressure helium gas over the rod surface and through a variable-length nozzle (*41*, *42*). The average nanocrystallite size was controlled by varying the delay time between the He gas pulse and the laser pulse or by changing the nozzle length. Because the surface-to-volume ratio of nanometer-scale materials is large, any dangling bonds at the nanocrystallite surface will act as traps to produce rapid nonradiative recombination of carriers, preventing light emission. After surface passivation of dangling bonds (with an HF etch and oxide regrowth process), a definite shift of the photoluminescence maximum to higher energy was seen as the mean particle size decreased (*41*). This is consistent with the behavior expected for light emission from carriers that are quantum confined in Si particles of 2 to 4 nm diameter, and TEM confirmed the existence of Si particles in this size range. More recently, deposits of Si nanocrystallites with diameters $\geq$ 3 nm were produced simply by excimer laser ablation of Si into constant-pressure (~2.5 to 10 mtorr) helium gas (*43*).

Nanocrystalline Si films currently are interesting because of questions about the origin of the relatively efficient visible light emission from porous and nanostructured Si samples (*44*), in contrast to the lack of visible emission from (indirect band gap) bulk Si samples. The relatively efficient light emission and the ability to shift its wavelength appear to be consequences of the films' nanocrystalline morphology. Thus, cluster-assembled nanocrystalline films of Si (and possibly other semiconductors) may provide an alternate route toward the development of visible electroluminescent devices, without the need for compound semiconductor lattice matching and heteroepitaxial growth.

The marriage of laser ablation with supersonic expansion techniques has also been used recently to create hybrid organic:inorganic films in which an organic material with high nonlinear optical activity [N-4-(4-nitrophenyl)-(s)-prolinol (NPP)] was encapsulated in small particles of silica ($SiO_2$) glass (*45*). The $SiO_2$ clusters were produced by laser ablation of an $SiO_2$ rod in a supersonic He expansion, and the organic vapor was entrained in a separate He gas pulse. A composite silica:NPP film was formed by mixing the two pulses and depositing the result on a nearby substrate. This technique is potentially valuable because it permits a thermally sensitive (organic) material with a desirable property (such as nonlinear optical activity) to be incorporated at room temperature in a low-loss photonic medium (silica glass) without degradation, thereby avoiding the problem of decomposition of organic compounds at normal glass-processing temperatures (*45*). Similar techniques can be used to form other exotic hybrid or composite thin films containing normally incompatible materials that would be difficult to synthesize otherwise.

## REFERENCES AND NOTES


1. H. M. Smith and A. F. Turner, *Appl. Opt.* **4**, 147 (1965).
2. D. Dijkkamp *et al.*, *Appl. Phys. Lett.* **51**, 619 (1987); X. D. Wu *et al.*, *ibid.*, p. 861.
3. See D. B. Chrisey and G. K. Hubler, Eds., *Pulsed Laser Deposition of Thin Films* (Wiley, New York, 1994).
4. The ablation plasma's formation, propagation, and interactions with ambient gas molecules have been studied extensively by Geohegan and co-workers [D. B. Geohegan, in (*3*), pp. 115–165].
5. Q. Li *et al.*, *Phys. Rev. Lett.* **64**, 3086 (1990); D. H. Lowndes *et al.*, *ibid.* **65**, 1160 (1990); J.-M. Triscone *et al.*, *ibid.* **64**, 804 (1990).
6. L. P. Lee, K. Char, M. S. Colclough, G. Zaharchuk, *Appl. Phys. Lett.* **59**, 3051 (1991).
7. For a detailed discussion of the mechanisms by which particulates are formed and methods to eliminate or minimize them, see L.-C. Chen, in (*3*), pp. 167–197.
8. The ablation "plume" actually consists of two components: the high-intensity, forward-peaked, stoichiometric part, plus a low-intensity, evaporative part, varying approximately as cos θ (the angle with respect to the sample normal, varying from −90° to 90°), that dominates at large deposition angles in vacuum [T. Venkatesan, X. D. Wu, A. Inam, J. B. Wachtman, *Appl. Phys. Lett.* **52**, 1193 (1988)]. Consequently, a small fraction of the deposited material is expected to be nonstoichiometric if beam scanning is used. The pragmatic solutions to this problem have been to operate at sufficiently high $E_d$ that the evaporative component is negligible, to use films grown mostly from the central plume region, or to combine these methods.
9. J. A. Greer and M. D. Tabat, *J. Vac. Sci. Technol. A* **13**, 1175 (1995).
10. S. Witanachchi, K. Ahmed, P. Sakthivel, P. Mukherjee, *Appl. Phys. Lett.* **66**, 1469 (1995); S. Witanachchi and P. Mukherjee, *J. Vac. Sci. Technol. A* **13**, 1171 (1995).
11. H. Sankur and J. T. Cheung [*Appl. Phys. A* **47**, 271 (1988)] first pointed out the particulate-free nature of ablation from a liquid target, but steady-state target melting generally is not practical because of the high vapor pressures of most liquids.
12. T. Kawai, Y. Egami, H. Tabata, S. Kawai, *Nature* **349**, 200 (1991).
13. X. Li, T. Kawai, S. Kawai, *Jpn. J. Appl. Phys.* **33**, L18 (1994).
14. D. P. Norton *et al.*, *Science* **265**, 2074 (1994).
15. H. Koinuma, M. Kawasaki, M. Yoshimoto, *Mater. Res. Soc. Symp. Proc.*, in press.
16. H. Koinuma, H. Nagata, T. Tsukahara, S. Gonda, M. Yoshimoto, *Appl. Phys. Lett.* **58**, 2027 (1991); M. Y. Chern, A. Gupta, B. W. Hussey, T. M. Shaw, *J. Vac. Sci. Technol. A* **11**, 637 (1993).
17. H. Tabata, H. Tanaka, T. Kawai, *Appl. Phys. Lett.* **65**, 1970 (1994).
18. T. M. Shaw *et al.*, *J. Mater. Res.* **9**, 2566 (1994).
19. H.-M. Christen *et al.*, *Appl. Phys. Lett.* **68**, 1488 (1996).
20. R. Ramesh *et al.*, in *Polycrystalline Thin Films: Structure, Texture, Properties and Applications*, K. Barmak *et al.*, Eds. (Materials Research Society, Pittsburgh, PA, 1994), pp. 431–443; R. Ramesh, O. Auciello, V. G. Keramides, R. Dat, in *Science and*

*Technology of Electroceramic Thin Films*, O. Auciello and R. Waser, Eds. (Kluwer Academic, Dordrecht, Netherlands, 1995), pp. 1–22.
21. The committee is chaired by H. Koinuma, Tokyo Institute of Technology.
22. S. Jin *et al.*, *Science* **264**, 413 (1994).
23. S. Jin *et al.*, *Appl. Phys. Lett.* **67**, 557 (1995).
24. E. E. Fullerton *et al.*, *ibid.* **63**, 1699 (1993).
25. D. R. McKenzie, D. Muller, B. A. Pailthorpe, *Phys. Rev. Lett.* **67**, 773 (1991).
26. S. D. Berger, D. R. McKenzie, P. J. Martin, *Philos. Mag. Lett.* **57**, 285 (1988).
27. F. Davanloo, E. M. Juengerman, D. R. Jander, T. J. Lee, C. B. Collins, *J. Appl. Phys.* **67**, 2081 (1990); C. B. Collins *et al.*, *ibid.* **69**, 7862 (1991); F. Davanloo *et al.*, *ibid.* **71**, 1446 (1992); C. B. Collins, F. Davanloo, T. J. Lee, H. Park, J. H. You, *J. Vac. Sci. Technol. B* **11**, 1936 (1993).
28. J. J. Cuomo, D. L. Pappas, J. Bruley, J. P. Doyle, K. L. Saenger, *J. Appl. Phys.* **70**, 1706 (1991).
29. D. L. Pappas *et al.*, *ibid.* **71**, 5675 (1992); D. L. Pappas, K. L. Saenger, J. J. Cuomo, R. W. Dreyfus, *ibid.* **72**, 3966 (1992).
30. F. Xiong, Y. Y. Wang, V. Leppert, R. P. H. Chang, *J. Mater. Res.* **8**, 2265 (1993); F. Xiong, Y. Y. Wang, R. P. H. Chang, *Phys. Rev. B* **48**, 8016 (1993).
31. A. A. Puretzky, D. B. Geohegan, G. E. Jellison Jr., M. M. McGibbon, in *Film Synthesis and Growth Using Energetic Beams*, H. A. Atwater, J. T. Dickinson, D. H. Lowndes, A. Polman, Eds. (Materials Research Society, Pittsburgh, PA, 1995), vol. 388, pp. 145–150; *Appl. Surf. Sci.* **96–98**, 859 (1996).
32. N. A. Marks, D. R. McKenzie, B. A. Pailthorpe, M. Bernasconi, M. Parrinello, *Phys. Rev. Lett.* **76**, 768 (1996).
33. See the recent review by J. E. Jaskie, *Mater. Res. Soc. Bull.* **21**, 59 (1996).
34. An intensified charge-coupled device (CCD)–array camera system coupled to a tunable (400 to 720 nm) narrow-band (full width at half maximum, 5 nm) liquid-crystal filter was used for species-resolved spectroscopic imaging. The ability to study simultaneously both fast- and slow-moving components of the ablation plume results from the extreme (photon counting) sensitivity of the intensified CCD-array camera system and its ability to collect photons from all wavelengths simultaneously. Slow-moving or scattered components of the laser-sputtered flux (such as redeposited material near the target) are not overlooked. For details and other examples of gated, species-resolved imaging, see (*4*) and D. B. Geohegan and A. A. Puretzky, *Mater. Res. Soc. Symp. Proc.*, in press.
35. D. Feiler, R. S. Williams, A. A. Talin, H. Yoon, M. S. Goorsky, *J. Cryst. Growth*, in press.
36. C. M. Rouleau *et al.*, *Appl. Phys. Lett.* **67**, 2545 (1995).
37. D. H. Lowndes *et al.*, *Mater. Res. Soc. Symp. Proc.*, in press.
38. C. M. Rouleau *et al.*, *ibid.*, in press.
39. Time-resolved ion current measurements during the ablation of various materials have revealed that over a limited range of ambient gas pressures, the ablation plume generally splits into two or more components that travel at different average velocities and KEs. For a detailed description of ion current measurements and the "plume splitting" phenomenon, see (*4*) and also D. B. Geohegan and A. A. Puretzky, *Appl. Phys. Lett.* **67**, 197 (1995); *Appl. Surf. Sci.* **96–98**, 131 (1996).
40. K.-D. Rinnen, K. D. Kolenbrander, A. M. DeSantolo, M. L. Mandich, *J. Chem. Phys.* **96**, 4088 (1992).
41. L. A. Chiu, A. A. Seraphin, K. D. Kolenbrander, *J. Electron. Mater.* **23**, 347 (1994).
42. Similar pulsed laser ablation supersonic expansion sources were first developed by Smalley and coworkers nearly 15 years ago [D. E. Powers *et al.*, *J. Phys. Chem.* **86**, 2556 (1982)].
43. T. Yoshida, S. Takeyama, Y. Yamada, K. Mutoh, *Appl. Phys. Lett.* **68**, 1772 (1996).
44. See L. Canham, *Mater. Res. Soc. Bull.* **18**, 22 (1993).
45. W. M. K. P. Wijekoon, M. Y. M. Lyktey, P. N. Prasad, J. F. Garvey, *Appl. Phys. Lett.* **67**, 1698 (1995).
46. This research was carried out at Oak Ridge National Laboratory (ORNL), managed by Lockheed Martin Energy Research Corporation for the U.S. Department of Energy under contract DE-AC05-96OR22464. C.M.R. was supported by an appointment to the ORNL Postdoctoral Research Associates Program administered jointly by ORNL and the Oak Ridge Institute for Science and Education.

# Chemical Solution Routes to Single-Crystal Thin Films

F. F. Lange

**Epitaxial thin films of inorganic single crystals can be grown on single-crystal substrates with a variety of different solution chemistries. This review emphasizes chemical solution deposition, in which a solution is used to deposit a layer of precursor molecules that decompose to low-density, polycrystalline films during heating. Ways to control film cracking during deposition and heat treatment and why many precursors synthesize metastable crystalline structures are discussed, and the different mechanisms that convert the polycrystalline film into a single crystal are reviewed. Hydrothermal epitaxy, in which single crystal thin films are directly synthesized on templating substrates in an aqueous solution at temperatures <150°C, is also discussed.**

Inorganic, single-crystal thin films can be produced from solution (either aqueous or organic) that contain precursor molecules for the different elements in the multielement compound of interest. Solution routes are relatively new and have been explored for possible device applications (such as nonvolatile memories, pyroelectric detectors, and field-emission displays) as an alternative to more costly vapor-phase routes (*1*). Oxide compositions, specifically those with unusual electro-optical properties, such as $LiNbO_3$ (*2*, *3*) and $Pb(Zr,Ti)O_3$ (*4*, *5*), and others including rare-earth aluminates (*6*), cuprate superconductors (*7*, *8*), and other oxides (*9*–*14*), have received most of the attention. Growth of single-crystal carbides (*15*), nitrides, and a limited group of metals is possible. As in the many different vapor-phase routes (*1*), single-crystal substrates are used as a supporting structure and a template for the oriented overgrowth of the film material—a process known as epitaxy.

The chemical solution deposition route to epitaxial films has received the most technical attention and will be the focus of this review. In this route, the solution is merely a vehicle to deposit, either by spin-coating or dip-coating, the desired elements onto a single-crystal substrate. A solid precursor film forms that decomposes (pyrolyzes) to a polycrystalline inorganic film during heating. The polycrystalline film converts to a single-crystal film at higher temperatures by one of a number of mechanisms described below. A number of different phenomena effect epitaxy. Different solution precursor chemistries can be used to produce the same inorganic material. The different precursor coatings can have different properties that include different rheological behaviors that influence coating coverage, different mechanical properties that affect cracking during processing, and different decomposition products that can alter the composition formed during pyrolysis. The large volume decrease produced during evaporation and pyrolysis will lead to the formation of "mud" cracks if the film thickness is greater than a critical value. Because the inorganic material is formed by pyrolysis at temperatures where diffusion is kinetically limited, metastable phases can crystallize to effect epitaxy during their transformation to the stable phase. In addition to these subjects, the effect of differences in crystal structure between the film and substrate on the epitaxy phenomena will also be reviewed.

In a second route, hydrothermal epitaxy, the single-crystal thin film is directly synthesized on a substrate in water at temperatures ≤150°C. This route only warrants a few paragraphs because it has just "seen the light of literature."

One advantage of solution routes is the economics that "beakers and benches" chemistry offer relative to capital-intensive vapor-phase routes. A second is the high degree of compositional control inherent with the solution synthesis of multielement, inorganic materials. Also, the newly introduced hydrothermal route offers processing temperatures that approach ambient conditions, which would be very advantageous for sequential processing of devices where

The author is in the Materials Department, University of California, Santa Barbara, CA 93106, USA.